Cell, Vol. 92, 819–828, March 20, 1998, Copyright ©1998 by Cell Press

Cotranslational Biogenesis of NF-κB p50 by the 26S Proteasome

Li Lin,*‡ George N. DeMartino,§ and Warner C. Greene*†‡‖

*Gladstone Institute of Virology and Immunology
†Department of Medicine
‡Department of Microbiology and Immunology
University of California
San Francisco, California 94141
§Department of Physiology
University of Texas Southwestern Medical Center
Dallas, Texas 75235

Summary

The NFKB1 gene encodes two functionally distinct proteins termed p50 and p105. p50 corresponds to the N terminus of p105 and with p65 (RelA) forms the prototypical NF-κB transcription factor complex. In contrast, p105 functions as a Rel-specific inhibitor (IκB) and has been proposed to be the precursor of p50. Our studies now demonstrate that p50 is generated by a unique cotranslational processing event involving the 26S proteasome, whereas cotranslational folding of sequences near the C terminus of p50 abrogates proteasome processing and leads to p105 production. These results indicate that p105 is not the precursor of p50 and reveal a novel mechanism of gene regulation that ensures the balanced production and independent function of the p50 and p105 proteins.

Introduction

The eukaryotic transcription factor, NF-κB, is a heterodimeric complex composed of two polypeptide subunits termed p50 and p65 (RelA). Normally, NF-κB is sequestered in the cytosol by a family of ankyrin motif-rich inhibitors termed the IκBs (Baeuerle and Baltimore, 1988). However, extracellular stimuli, including tumor necrosis factor α (TNFα), lipopolysaccharide (LPS), and phorbol esters, lead to the nuclear expression of NF-κB (for review, Baeuerle and Henkel, 1994; Siebenlist et al., 1994; Thanos and Maniatis, 1995; Verma et al., 1995; Baeuerle and Baltimore, 1996; Baldwin, 1996), which in turn regulates an array of genes involved in immune, inflammatory, and antiapoptotic responses (Beg et al., 1995; Sha et al., 1995; Beg and Baltimore, 1996; Van Antwerp et al., 1996; Wang et al., 1996).

The p105 protein is encoded by the NFKB1 gene (Ghosh et al., 1990; Kieran et al., 1990). The N-terminal portion of p105 corresponds to the p50 subunit of the prototypical NF-κB complex. These p50 molecules either assemble with other Rel family members, including p65 and c-Rel, or alternatively self-assemble as homodimers (Henkel et al., 1992; Rice et al., 1992; Naumann et al., 1993). The C-terminal portion of p105 is remarkable for the presence of ankyrin repeats resembling those present in IκB-α. In this regard, p105 binds to and sequesters other Rel-related proteins in the cytoplasm, thereby functioning as an IκB (Rice et al., 1992). Thus, despite sharing an identical N-terminal Rel homology domain, p50 and p105 subserve quite different biological functions in the cell.

Like IκB-α, p105 is basally phosphorylated and undergoes additional phosphorylation upon cellular stimulation (Mercurio et al., 1993; Naumann and Scheidereit, 1994; MacKichan et al., 1996). However, unlike the signal-coupled phosphorylation of serines 32 and 36 in IκB-α (Lin et al., 1995; Traenckner et al., 1995), which leads to the degradation of this inhibitor within the 26S proteasome (Henkel et al., 1993; Chen et al., 1995; Scherer et al., 1995), phosphorylation of the C terminus of p105 produces no clear functional consequences. Mitogenic stimuli have been reported to moderately increase p50 expression (Mercurio et al., 1993; Donald et al., 1995); however, large amounts of p50 are present in unstimulated cells, suggesting that mitogenic stimulation is not obligately required for p50 generation. Additionally, the candidate oncoprotein BCL-3 induces p50 homodimers from cytosolic p105/p50 complexes without enhancing the processing of p105 (Watanabe et al., 1997). Finally, a glycine-rich region (GRR) between amino acids 375-401 in p105 is required for p50 generation both in COS cells (Lin and Ghosh, 1996) and rabbit reticulocyte lysates (Lin and Greene, unpublished data). Of note, sequences downstream of the GRR can be replaced with heterologous elements (Betts and Nabel, 1996; Lin and Ghosh, 1996), suggesting that this region does not contain sequence-specific elements required for p50 production.

The generation of p50 appears to involve the 26S proteasome as first indicated by the requirement for ATP (Fan and Maniatis, 1991) and later by the use of proteasome inhibitors (Palombella et al., 1994). Generation of p50 is also defective in a yeast strain mutated in the PRE1 proteasome subunit gene (Palombella et al., 1994). Thus far, p105 and perhaps the closely related NFKB2 gene product, p100, are the only examples of proteasome substrates that are processed rather than completely degraded. How the N-terminal portion of p105 is spared from complete degradation by the proteasome remains an enigma.

We now describe a series of studies demonstrating that full-length p105 is not the primary precursor of p50. Rather, p50 is generated cotranslationally by a proteasome-mediated process that ensures the production of both p50 and p105 and preserves their independent functions. Our results further suggest that cotranslational folding of the N-terminal portion of p105 protects this region that forms p50 from degradation by the proteasome, whereas folding of sequences downstream of the GRR precludes processing altogether, leading to p105 production. These findings highlight a previously unrecognized mechanism of gene regulation in mammalian cells and provide a natural example for the proposed sequential and cotranslational folding of eukaryotic proteins (Netzer and Hartl, 1997).

‖To whom correspondence should be addressed.

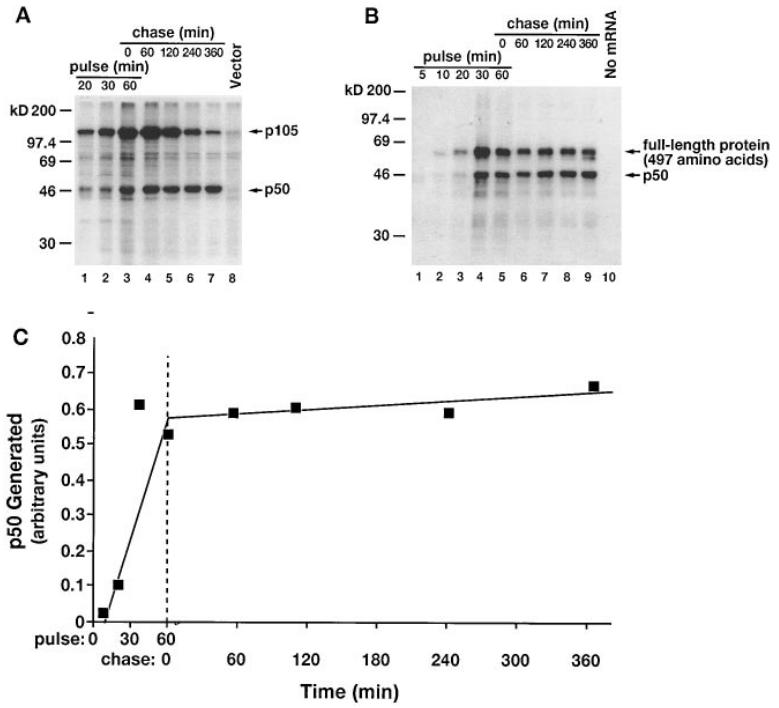

Figure 1. Pulse-Chase Studies of p50 Generation

(A) Pulse-chase analysis of p50 generation in vivo. CHO-CD14 cells transfected with p105 expression vector DNA were pulse-radiolabeled with [^{35}S]methionine/cysteine and chased for the time periods indicated. The 1 hr pulse radiolabeling point was regarded as time 0 for the chase (lane 3).

(B) Pulse-chase analysis of p50 generation in vitro. mRNA encoding the N-terminal 497 amino acids of p105 was used to program translation in rabbit reticulocyte lysates.

(C) Densitometry analysis of the time course of p50 generation. Production of p50 was assessed by densitometry throughout the time course of the in vitro pulse-chase study.

Results

NF-κB p105 and p50 Do Not Exhibit a Classical Precursor–Product Relationship in Pulse-Chase Radiolabeling Studies

Earlier studies suggested a precursor–product relationship between p105 and p50 either in the absence (Fan and Maniatis, 1991) or presence of mitogen stimulation (Mercurio et al., 1993; Donald et al., 1995; Rousset et al., 1996). However, the generation of p50 was slow and substantial quantities of p50 were evident before the initiation of chase in these studies. To assess the relationship between p105 and p50 further, we performed pulse-chase radiolabeling experiments in CHO-CD14 cells transfected with a mouse p105 cDNA expression vector, harvesting multiple samples during both pulse and chase periods (Figure 1A). Increasing amounts of both p105 and p50 were readily detected at each of pulse radiolabeling time points (lanes 1–3). Even though p105 levels declined during the 6 hr chase period, no corresponding increase in p50 radiolabeling was detected (lanes 4–7). Similarly, in pulse-chase studies performed in vitro using rabbit reticulocyte lysates programmed with mRNA encoding a 497–amino acid fragment of p105, we observed essentially simultaneous radiolabeling of p50 and the larger polypeptide during the initial pulse radiolabeling phase (Figure 1B, lanes 3–5). Additionally, the radiolabel present in the 497–amino acid protein did not chase to p50 during the subsequent 6 hr incubation period. Densitometric analyses of the production of p50 in these in vitro (Figure 1C) and in vivo (data not shown) studies indicate that p50 is rapidly generated during the pulse period but only slowly accumulates during the subsequent chase. The disappearance of p105 during the chase phase of the in vivo studies (Figure 1A) was not accompanied by an increase in p50 and thus appears to result from the degradation of p105, as previously suggested (Harhaj et al., 1996), rather than processing to p50. These findings suggested that the generation of p50 may be closely linked with translation.

A Nascent but Not Folded 497–Amino Acid Fragment of p105 Is Sufficient to Generate p50

Although the C-terminal portion of p105 can be substituted with foreign sequences without affecting p50 generation (Betts and Nabel, 1996; Lin and Ghosh, 1996), we tested whether the same 497–amino acid fragment used in in vitro translation was processed in vivo. Surprisingly, even though the full-length 497–amino acid protein was stably expressed in CHO-CD14 cells and p105 was normally processed to p50 (Figure 2B, lane 1), virtually no p50 was generated from p-497 (Figure 2B, lane 2). This lack of processing of the 497–amino acid fragment in vivo thus differed sharply from the results obtained with this same fragment in vitro (Figure 1B). Both vectors expressed the same 497–amino acid polypeptide; however, p-497 contained a stop codon following residue 497, while the mRNA used in in vitro expression was truncated by restriction of the DNA template with XhoI prior to transcription.

To determine whether the observed differences in p50 generation in vivo and in vitro reflected the presence or absence of a stop codon, the p-497/XhoI fragment was reengineered with a stop codon (p-497/Stop) and tested for p50 generation in vitro. As shown in Figure 2C (lane 2), the 497–amino acid protein translated from an mRNA containing a stop codon yielded little p50. In contrast and as shown previously, significant amounts of p50 were generated from mRNA derived from the p-497/XhoI vector (Figure 2C, lane 1).

These findings are revealing because in the absence

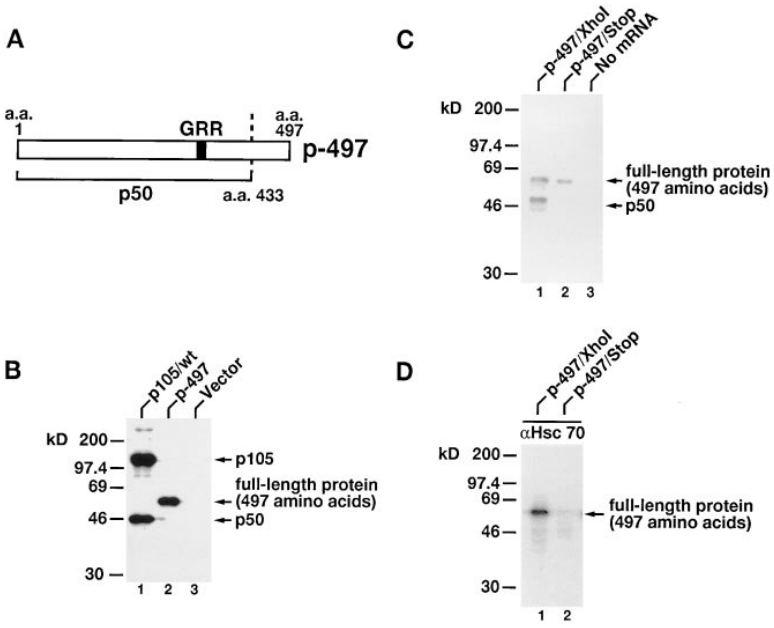

Figure 2. Differential Processing of a 497-Amino Acid N-terminal Fragment of p105 from mRNAs Containing or Lacking a Translation Stop Codon

(A) Diagram of the 497–amino acid p105 N-terminal fragment employed in the study. The fragment contains the glycine-rich region (GRR) and spans beyond the estimated C terminus of p50 located at residue 433.

(B) Expression and processing of p105 versus the 497–amino acid N-terminal fragment of p105 in vivo. T7 gp*10* epitope–tagged p105 and p-497 were transfected into CHO-CD14 cells and radiolabeled as described in Figure 1. Lysates were prepared and immunoprecipitated. Lane 1, wild-type p105; lane 2, the 497–amino acid fragment of p105; lane 3, control cells transfected with empty vector.

(C) In vitro translation of the p105-derived 497–amino acid fragment from mRNAs either lacking or containing a translation stop codon. The two mRNAs derived from p-497/XhoI (lane 1, lacking a stop codon) or p-497/Stop (lane 2, containing a stop codon) were translated in rabbit reticulocyte lysates, and the protein products from both translations were immunoprecipitated with anti-p105 specific antisera. Lane 3, immunoprecipitation of control lysates not programmed with mRNA.

(D) The Hsc70 chaperone binds to the nascent but not folded form of the 497–amino acid fragment of p105. mRNAs lacking (lane 1) or containing (lane 2) a stop codon following the N-terminal 497 amino acids of p105 were translated in rabbit reticulocyte lysates. Translation was synchronized by the addition of ATCA (75 mM, final concentration) 3 min after initiation. The arrow indicates coimmunoprecipitation of the 497–amino acid fragment of p105 translated from an mRNA lacking a stop codon by antibodies specific for Hsc 70.

of a stop codon, the ribosome stalls at the end of the mRNA and the nascent polypeptide remains bound to the ribosome as a peptidyl tRNA (Krieg et al., 1989). In addition, this peptide fails to undergo posttranslational folding (Frydman et al., 1994). Elimination of stop codons has been used to study the folding of nascent polypeptides and their interactions with molecular chaperones (Frydman et al., 1994; Hansen et al., 1994; Frydman and Hartl, 1996; Komar et al., 1997). To verify that the 497–amino acid fragment lacking the stop codon was in a nascent state, aurintricarboxylic acid (ATCA) synchronized in vitro translations (Stewart et al., 1971; Frydman et al., 1994) were performed and the protein products immunoprecipitated with an antibody specific for the Hsc70 chaperone. Hsc70 exhibits high affinity for nascent or unfolded polypeptides but binds poorly to folded proteins (Beckmann et al., 1990). As shown in Figure 2D, the anti-Hsc70 coimmunoprecipitated the 497–amino acid fragment derived from p-497/XhoI but did not coimmunoprecipitate the 497–amino acid fragment produced from p-497/Stop. The anti-Hsc70 antibody also did not coimmunoprecipitate the p50 protein generated from the nascent 497–amino acid fragment (Figure 2D, lane 1), suggesting that this product is rapidly folded. Together, these results indicate that premature release and folding of a 497–amino acid fragment of p105 abolishes the generation of p50. In contrast, the same polypeptide efficiently generates p50 if it remains nascent.

Translation beyond Amino Acid 497 of p105 Permits the Generation of p50

Since wild-type p105 generates p50, we reasoned that continuing translation beyond amino acid 497 should allow the generation of p50. To determine how much additional translation is required for p50 production, we moved the stop codon progressively downstream of residue 497 and tested these p105-derived fragments in vivo (Figure 3B) and in vitro (Figure 3C) for p50 production. An overview of p105 with various landmarks is provided in Figure 3A. As expected, p105 mRNAs terminating after residue 481 or 497 did not support p50 generation (Figure 3B, lanes 2 and 3). Similarly, repositioning of the stop codon following residue 504, 509, or 514 did not lead to significant p50 production in vivo (Figure 3B, lanes 4–6). However, introduction of the stop codon after residue 530 or further downstream resulted in significant p50 accumulation (lanes 7–9). When a similar "stop codon scan" was carried out in vitro, insertion of the stop codon after residue 514 supported p50 generation (Figure 3C, lane 3). We suspect that the different boundaries obtained in the in vivo and in vitro assays (residue 530 vs. 514) may stem from the slower rate of translation and protein folding that occurs in vitro. Of note, Fan and Maniatis (1991) similarly observed that a human p105 deletion mutant terminating at residue 504 failed to generate p50 in transfected COS cells. Together, these results indicate that in the natural situation, continuing translation to a point approximately 100 amino acids beyond the C terminus of p50 (residue 433; Lin and Ghosh, 1996) is required for the generation of p50.

p50 Is Generated Prior to Completion of Translation of Full-Length p105

To test further the possibility of cotranslational production of p50, ATCA synchronized in vitro translations were performed for specific periods of time, followed by the addition of puromycin to interrupt further translational

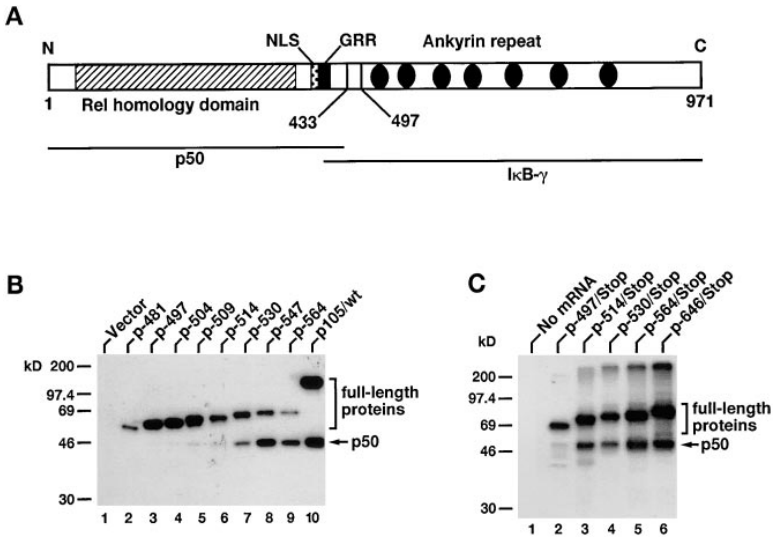

Figure 3. A Stop Codon Scan of p105

(A) Overview of the mouse p105 protein. Known functional domains and relevant amino acids are indicated.

(B) Stop codon scanning to evaluate p105 processing in vivo. Different C-terminal deletions of p105 were prepared by inserting stop codons between residues 481 and 564. These constructs were expressed in CHO-CD14 cells and analyzed for processing to p50 by immunoblotting. Lane 1 depicts results obtained with vector DNA, while lane 10 shows the results obtained with wild-type p105. The name of each experimental plasmid indicates the number of N-terminal residues of p105 present in the resultant protein.

(C) Stop codon scanning to evaluate p105 processing in vitro. p105 cDNAs containing a nested set of progressive 3′ deletions followed by a stop codon were transcribed and translated in rabbit reticulocyte lysates and immunoprecipitated with anti-p105 (NLS) antibody. The name of each plasmid indicates the number of N-terminal residues present in the p105-derived fragment.

elongation (Blobel and Sabatini, 1971). To separate p50 generation and the completion of translation temporally, a 646–amino acid version of p105 and a translation temperature of 25°C were selected. Under these conditions, translation proceeded at an average rate of 60 amino acids per min, similar to that observed in prior studies with luciferase (Frydman et al., 1994). In these synchronized translations, p50 production was observed at 9 min, indicating the synthesis of approximately 540 amino acids (Figure 4, lane 7). In contrast, translation of the larger 646–amino acid fragment required approximately 11 min (Figure 4, lane 10). Thus, the generation of p50 occurs well before complete synthesis of the p105-derived fragment. Similar results were obtained using a 781–amino acid fragment of p105 (data not shown).

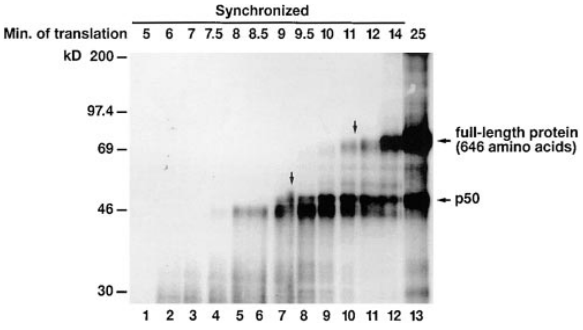

Figure 4. NF-κB p50 Is Generated Prior to the Synthesis of the Full-Length Protein

An mRNA encoding a 617–amino acid p105 N-terminal fragment plus an N-terminal T7 gp*10* and C-terminal His epitope tag (646 total amino acids) was used to program translation in rabbit reticulocyte lysates. The time points when p50 and the full-length protein were first detected are indicated by vertical arrows (lane 7, 9 min for p50; lane 10, 11 min for the full-length protein). An immunoreactive fragment slightly smaller than p50 was noted at 8 min (lane 5), which gradually diminished at later time points. This product could represent an aberrantly processed form of p50 resulting from the interruption of translation. The control shown in lane 13 corresponds to an unsynchronized translation performed at 25°C for 25 min and immunoprecipitated identically to the other samples.

Cotranslational Biogenesis of p105 and p50 Is Influenced by Sequences Located Downstream of the GRR

In most cells, p105 and p50 are produced in nearly equivalent amounts (Naumann et al., 1993; Lin and Ghosh, 1996). Similarly, the nascent 497–amino acid fragment is not completely processed to p50 but rather yields a roughly balanced ratio of the two proteins (Figure 2C, lane 1). This incomplete processing raises the possibility that this process may be stochastic in nature. Since folding of nascent polypeptides occurs cotranslationally and the N-terminal portion of a protein may adopt a native conformation before the completion of C-terminal synthesis (Komar et al., 1997), it seemed possible that such cotranslational folding of p105 might influence the ratio of the products generated. A prior study has shown that replacement of the entire C terminus of p105 with T7 gp*10* or IκB-α enhances p50 generation (Lin and Ghosh, 1996). To test whether sequences immediately surrounding the C terminus of p50 (approximately residue 433) might influence the ratio of p50 and p105 production, we fused the N-terminal region of either the T7 gp*10* or the IκB-α genes to the GRR ending at residue 401 to generate 497–amino acid fusion proteins (Figure 5A). Since these gene products contain different 96–amino acid sequences between the GRR and the C terminus, their local propensity to fold cotranslationally might vary and be reflected by differences in p50 generation. Expression of the p50/Δgp*10* chimeric protein in CHO-CD14 cells revealed markedly enhanced generation of p50 compared to p-497, which generated very little p50 (Figure 5B, compare lanes 2 and 4). Substitution of the same segment with 96 amino acids from IκB-α moderately enhanced p50 generation (compare lanes 2 and 6). To exclude the possibility that these observed

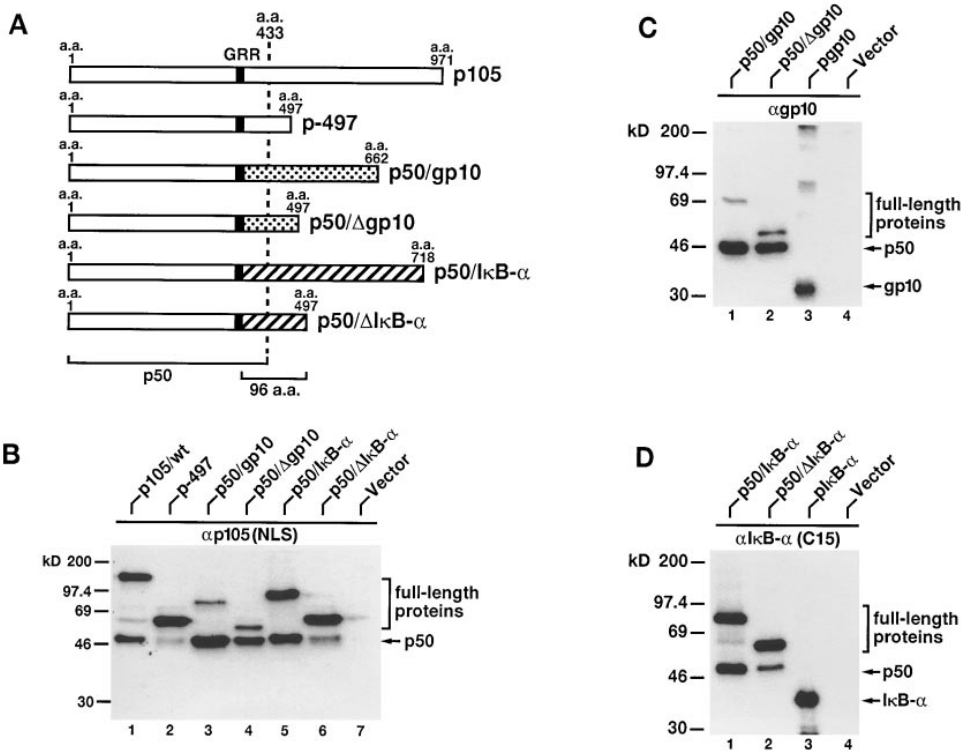

Figure 5. Sequences Positioned Downstream of the p105 GRR Modulate the Ratio of p50 and p105 Production

(A) Diagram of the various chimeric proteins prepared and analyzed in these studies. The gp*10* and IκB-α peptide fragments fused in-frame distal to the GRR of p105, and their lengths are indicated respectively by the cross-hatching and stripes.

(B) Generation of p50 from the different chimera constructs. Each of the chimeras was expressed in CHO-CD14 cells, and the subsequent lysates were analyzed by immunoblotting using the anti-p105 (NLS) antibody. The p50 Δgp*10* full-length protein migrated slightly faster than the 497 residue fragment of p105, presumably due to its different amino acid composition.

(C) Immunoblotting of the p50/gp*10*-derived lysates with anti-gp*10* antibody. The control full-length gp*10* protein (345 amino acids) expressed in CHO-CD14 cells is shown in lane 3, while results obtained with the empty vector control are shown in lane 4.

(D) Immunoblotting of the p50/IκB-α-derived lysates with antibodies specific for the N terminus of IκB-α (C-15). Control recombinant IκB-α protein expressed in *E. coli* is shown in lane 3 and the empty vector control in lane 4.

differences in p50 generation reflected different reactivity of the chimeras with the anti-p50 antibody, the extracts from the p50/Δgp*10* and p50/ΔIκB-α transfected cells were immunoblotted with antibodies specific for gp*10* and IκB-α, respectively (Figures 5C and 5D). These studies confirmed enhanced generation of p50 with both chimeric proteins (compare lane 2 of Figure 5B with Figures 5C and 5D). Thus, changing the amino acid in the 96–amino acid segment that adjoins the GRR and encompasses the C terminus of p50 and additional downstream sequences likely alters the folding of this region and influences the stochastic process that determines the ratio of p50 and p105 produced.

The 26S Proteasome Mediates Cotranslational Processing of p105

We next examined the involvement of the 26S proteasome in the cotranslational generation of p50. Production of p50 was studied in the presence of a *Streptomyces noursei*–derived metabolite lactacystin, which is a highly specific proteasome inhibitor (Fenteany et al., 1994; Jensen et al., 1995; Craiu et al., 1997). The potent *clasto*-lactacystin β-lactone derivative of lactacystin was used in these experiments because it corresponds to the biologically active form of this inhibitor (Dick et al., 1996, 1997). The addition of *clasto*-lactacystin β-lactone at concentrations as low as 10 μM inhibited the generation of p50 while not altering the production of p105 (Figure 6, compare lanes 1–4 with lanes 5–8). When added at the same concentration, *clasto*-lactacystin β-lactone also inhibited LPS-induced degradation of IκB-α in the CHO-CD14 cells (data not shown).

To detect a potential direct interaction of p105 with the proteasome, CHO-CD14 cells were transfected with p105, p-497, or p50 expression vectors containing a T7 gp*10* immunoepitope followed by pulse radiolabeling with [^{35}S]methionine/cysteine for 1 hr and chasing for 30 min. Radiolabeling was performed both in the presence and absence of the MG115 proteasome inhibitor. The lysates from these transfections were immunoprecipitated either with anti-gp*10* or E446-1, an antibody that reacts with the 20S proteasome. As shown in lane 8 of Figure 7, E446-1 effectively coimmunoprecipitated p105 but very little p50. However, newly synthesized p50 encoded by a p50 expression vector was effectively coimmunoprecipitated by the E446-1 antibody (lane 12), suggesting that the interaction of p105 fragments with the proteasome may occur during translation. The 497–

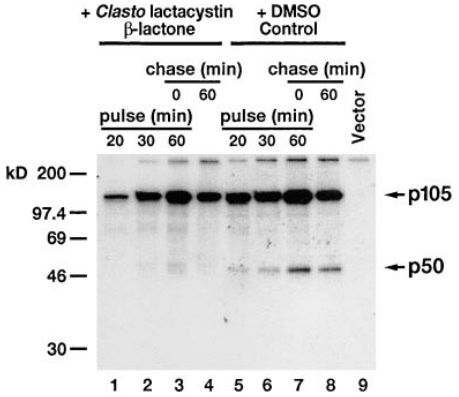

Figure 6. Cotranslational Generation of p50 Is Blocked by a Specific Inhibitor of the Proteasome

CHO-CD14 cells were transfected with a p105 expression vector containing an N-terminal gp*10* epitope tag. Cells were pretreated with 10 mM *clasto*-lactacystin β-lactone (lanes 1–4) or DMSO control (lanes 5–8) for 1 hr before pulse radiolabeling for 20–60 min and chasing for 0–60 min. The resultant cell lysates were immunoprecipitated by anti-gp*10* followed by 10% SDS-PAGE. The proteasome inhibitor was present throughout the course of the experiment. Lane 9 depicts results obtained with lysates from cells transfected with empty vector DNA.

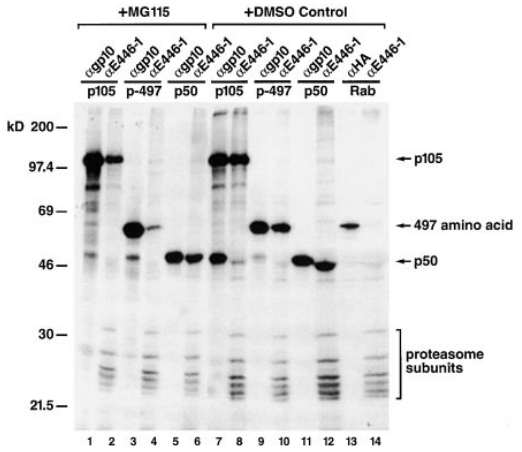

Figure 7. Physical Association of p105 and Its Various Fragments with the Proteasome

N-terminal gp*10* epitope–tagged expression vectors encoding p105 or various C-terminal deletions were transfected into CHO-CD14 cells. After 24 hr, aliquots of cells were incubated with the MG115 proteasome inhibitor or DMSO. The cells were then pulse-radiolabeled with [^{35}S]methionine/cysteine and chased in the presence of cycloheximide. Lysates were immunoprecipitated with either anti-gp*10* or antibodies specific for the 20S proteasome (E446-1). Three times the volume of the E446-1 immunoprecipitates was loaded to visualize the radiolabeled proteasome subunits. Samples shown in lanes 1–6 were prepared from cultures containing the MG115 proteasome inhibitor, while samples shown in lanes 7–12 were prepared in the absence of MG115. In lane 12, the p50 fragment immunoprecipitated by E446-1 migrated slightly more rapidly than the sample immunoprecipitated by anti-p105 (NLS) (line 11), likely reflecting an imperfection in the gel. The same protein exhibited normal migration in lane 6. The hemagglutinin-tagged HIV Rev-associated binding protein (Rab, approximately 60 kD including its epitope tag) was employed as a specificity control (lanes 13–14).

amino acid fragment of p105, although not generating p50, was still coimmunoprecipitated by E446-1 (lanes 4 and 10). These interactions of the p105 fragments with the proteasome appeared to be specific because control Rab (HIV Rev-associated binding protein) did not coimmunoprecipitate with the E446-1 antibody (lane 14), despite being stably expressed (lane 13). Of note, the physical association of p105 with the proteasome persists in the presence of the MG115 inhibitor (lanes 1–6), suggesting that the binding of p105 is independent of the proteolytic activity of the proteasome.

Discussion

NF-κB p50 Is Cotranslationally Generated by the 26S Proteasome

Several lines of evidence have emerged from our studies indicating that p50 is generated by a cotranslational mechanism. First, ribosome halting produced by elimination of the stop codon in an mRNA encoding a 497–amino acid fragment of p105 results in significant production of p50. In contrast, introduction of a stop codon into this same mRNA sharply inhibits p50 generation (Figure 2). These findings suggest that retention of the 497–amino acid polypeptide on the ribosome suspends the polypeptide in an extended, relatively unfolded state that promotes the generation of p50 (see model in Figure 8A). In contrast, premature release of this 497-residue polypeptide from the ribosome allows its complete folding, which effectively abrogates p50 production.

Second, progressive repositioning of the stop codon in the p105 mRNA revealed that translation to a point between amino acids 514 and 530 permitted p50 generation to occur in vivo (Figure 3). Relating this finding to the results obtained in the ribosome-halting experiment (Figure 2), we suggest that the time, rather than distance, of translation is likely the critical factor. Continuing translation to amino acid 530, like the absence of a stop codon, maintains an extended region in the nascent polypeptide for a sufficient period of time to allow proteasome processing to p50 (see model in Figure 8B). Third, to confirm the cotranslational nature of this process, we demonstrated in synchronized in vitro translation studies that p50 was produced prior to the completion of translation of the full-length protein (Figure 4). Finally, in sucrose gradient sedimentation studies, the in vitro translated nascent full-length polypeptides were detected in the dense ribosome-containing fractions, whereas p50 was present in the less dense top fractions, indicating that p50 was generated while the full-length fragment was still a peptidyl-tRNA (data not shown).

Our studies have clearly implicated the 26S proteasome in this cotranslational processing event. Addition of the proteasome-specific inhibitor, *clasto*-lactacystin β-lactone, blocked the generation of p50. Prior studies have demonstrated that replacement of C-terminal p105 sequences located downstream of the GRR have little effect on p50 generation (Betts and Nabel, 1996; Lin and Ghosh, 1996). Our results now provide a potential explanation for these results. Although the proteasome exclusively utilizes substrates that are unfolded, the particular structure of the nascent p105 fragment may make it an acceptable substrate for the proteasome. Specifically, the loosely structured GRR may form a proximal

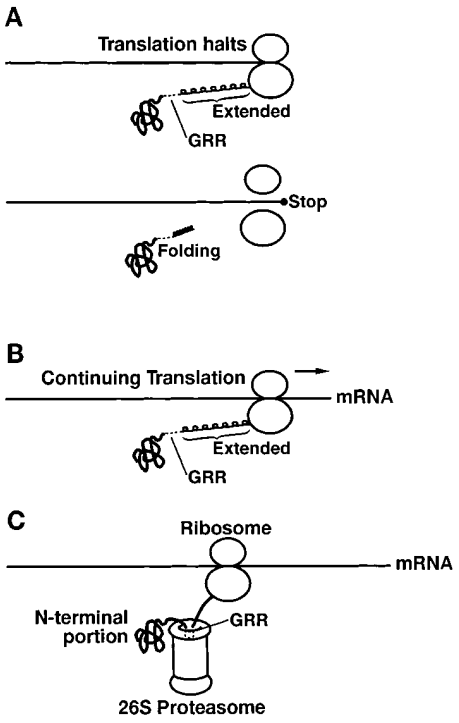

Figure 8. A Model for Cotranslational Biogenesis of p50 by the Proteasome

(A) Ribosome halting sustains an extended region in the nascent 497-residue p105-derived fragment allowing the generation of p50. In contrast to the effects of such ribosome halting (top) that allows proteasome-mediated processing, premature release of the p105-derived fragment from the ribosome by addition of a stop codon promotes rapid folding of the polypeptide and thus prevents its processing to p50 by the proteasome (bottom).

(B) Continuing translation is required for p50 generation. In the native situation, continuing translation serves to sustain an extended region in nascent p105 thereby allowing processing by the proteasome to proceed.

(C) The nascent p105 polypeptide may enter the proteasome as a loop to allow the processing. The loosely structured GRR in the nascent polypeptide, as well as downstream sequences displayed in an extended form due to continuing translation, may form a loop that is inserted through the narrow entrance of the proteasome allowing processing in the proteasome to proceed leading to p50 generation. Folding of this region blocks access to the proteasome and leads to p105 production. Similarly, cotranslational folding of the N-terminal portion of p105 may preclude its degradation by the proteasome.

portion of a peptide loop that inserts through the 13-Å diameter orifice of the proteasome into its barrel, allowing processing to proceed (see model in Figure 8C; for structure of the proteasome, Goldberg, 1995; Löwe et al., 1995; Weissman et al., 1995).

It remains unclear whether translation of the C terminus of p105 continues or is interrupted when p50 is produced. Despite extensive efforts, the C-terminal fragment of the processed NF-κB1 gene product has never been detected (Hatada et al., 1992; Lin and Greene, unpublished data). While a C-terminal fragment, termed IκB-γ, has been detected in certain mouse B cell lines, this protein is apparently produced by alternate mRNA splicing rather than p105 processing (Inoue et al., 1992; Liou et al., 1992). Lack of detection of the C terminus of p105 during p50 generation could be explained in one of two ways. First, translation of the C terminus of p105 may be interrupted during proteasome-mediated processing of p50, and thus the C terminus is never made. Second, the C terminus may be translated, but it may be continuously channeled into the barrel of the proteasome and rapidly degraded.

NF-κB p105 and p50 Do Not Exhibit a Precursor–Product Relationship

The pulse-chase radiolabeling studies (Figure 1) and our other findings clearly argue against a classical precursor–product relationship for p105 and p50. Functional studies of p105 and p50 have highlighted their different biological functions within the cell, with p50 acting as a Rel-related transcription factor (Ghosh et al., 1990; Kieran et al., 1990) and p105 serving as a specific cytoplasmic inhibitor of Rel proteins (Rice et al., 1992; Naumann et al., 1993). In contrast to Rel complexes sequestered by IκB-α in which this inhibitor is subject to signal-induced complete degradation by the proteasome (Henkel et al., 1993; Chen et al., 1995; Lin et al., 1995; Traenckner et al., 1995), Rel complexes sequestered by p105 are not rapidly mobilized to the nucleus in response to these same signals (Mercurio et al., 1993; Sun et al., 1994; Donald et al., 1995). While the biological function of these Rel-p105 complexes remains to be elucidated, the candidate oncoprotein BCL-3 may mobilize p50 molecules bound to p105 without enhancing p105 processing (Watanabe et al., 1997), suggesting that p105/p50 complexes could function as a source of p50 homodimers. Our studies now reveal how the independent functions of p105 and p50 are preserved through a novel cotranslational strategy that guarantees the production of both proteins. Although usually balanced, we have noted that the relative ratio of these two products can be influenced by either changes in the intrinsic structure of the protein as shown in Figure 5 or extrinsic changes in the intracellular environment; for example, increasing the pH of the growth medium enhances p105 production (data not shown). Overall, we suggest that these elements affect the "stochastic capture" of the polypeptide by the proteasome, which is influenced by the degree of protein folding and the rate of translation of p105.

In contrast to our studies incorporating both in vitro and in vivo approaches, the generation of p50 has previously been suggested based on in vitro analyses to involve posttranslational processing of p105 (Palombella et al., 1994). We suspect that the biological basis for p50 generation in the previous experimental setting (Palombella et al., 1994; Orian et al., 1995) and our system are in fact rather similar. Specifically, the in vitro system utilized in the earlier studies may promote a significant degree of posttranslational unfolding that recapitulates the conformation of the nascent polypeptide, thereby allowing processing by the 26S proteasome. Whereas ubiquitination is required for the observed posttranslational processing of p105 (Palombella et al., 1994; Orian et al., 1995), it is not clear whether ubiquitin plays any requisite role in the cotranslational processing that we have described.

How Is the GRR Involved in Cotranslational Generation of p50?

A 23–amino acid glycine-rich region (GRR) was previously identified as a critical element for the generation of p50 (Lin and Ghosh, 1996). Consistent with this observation, we have found that deletion of the GRR in nascent p105-derived fragments results in the generation of little or no p50 (data not shown). These findings thus demonstrate that the GRR is required for the cotranslational generation of p50. However, our studies have further shown that p105 proteins lacking the GRR continue to associate with the proteasome (data not shown), indicating that this element does not function as a primary proteasome targeting signal. While it is clear that many proteins are directed to the proteasome for degradation, emerging evidence suggests that some proteins may be targeted by virtue of a chaperone-like activity of the proteasome (Goldberg, 1995). As previously demonstrated, the GRR effectively functions in the context of certain heterologous proteins (gp*10*-GRR-GST chimera; Lin and Ghosh, 1996), whereas in other protein contexts (GST-GRR-gp*10*), no processing occurs (Lin and Greene, unpublished data). This latter result may reflect a diminished affinity of the N terminus of this protein for the proteasome.

NF-κB p105 as a Natural Model of Sequential and Cotranslational Protein Folding in Eukaryotes

Recently, Netzer and Hartl (1997) have proposed that eukaryotic proteins undergo sequential and cotranslational folding. In contrast, prokaryotic proteins seem to rely predominantly on a posttranslational mechanism of folding for the acquisition of full biological function. These conclusions derive from the analysis of a fusion protein containing a human H-Ras domain at the N terminus joined by a glycine-rich segment to a mouse dihydrofolate reductase (DHFR) domain at the C terminus. In these studies, the H-Ras domain was found to fold prior to synthesis of the DHFR polypeptide. Like this artificial fusion protein, p105 contains two functionally independent domains linked by the GRR. Further, p50 is generated from the N terminus prior to the completion of C-terminal translation. We suspect that the N-terminal Rel homology domain within p50 may undergo cotranslational folding and thus allow this region of the protein to escape proteasome-mediated degradation. Additionally, such N-terminal folding may also promote rapid downstream folding (as supported by stop codon scan experiments shown in Figure 3), leading to the production of p105 rather than p50. Evolutionarily, the different functions of the N- and C-terminal regions of p105 suggest that this protein may have been the result of a gene-fusion event and that the different functions of these two domains are preserved by a novel strategy involving cotranslational folding. The p105 protein certainly represents an interesting natural model to explore the sequential and cotranslational folding of eukaryotic proteins.

A Possible Novel Function of the 26S Proteasome

The proteasome is responsible for the constitutive degradation of most intracellular proteins in mammalian cells and for the selective degradation of certain proteins under specific physiological conditions (for reviews, Rechsteiner et al., 1993; Goldberg, 1995; Jentsch and Schlenker, 1995). These functions invariably involve the complete destruction of the target proteins. In contrast, for p105, cotranslational processing by the proteasome yields p50. Nascent p105 fragments may be prone to proteasome-mediated proteolysis for any of several reasons. For example, these nascent forms might be particularly susceptible to ubiquitination, thereby becoming preferential targets for the 26S proteasome like many other ubiquitinated proteins. The 26S proteasome corresponds to a complex consisting of the 20S proteasome and PA700 (also termed the 19S complex), which contains ATPases, a polyubiquitin binding protein, and other regulatory proteins (Ma et al., 1994). Alternatively, the 26S proteasome may function as a chaperone that interacts directly with nonubiquitinated forms of nascent p105. This interaction may retain a portion of p105 in an unfolded conformation that favors proteolysis. Roles for chaperone activity of the 26S proteasome have been hypothesized previously (Goldberg, 1995) but usually in the context of ATP-dependent unfolding of the substrate after it has been targeted to the 26S proteasome by ubiquitination. Recently, however, we have obtained direct evidence for chaperone activity of isolated PA700 with nonubiquitinated misfolded proteins (DeMartino and Thomas, unpublished data). Such results are consistent with a direct interaction of the 26S proteasome with nascent forms of p105. Thus, even though our experiments have utilized inhibitors and antibodies against the 20S proteasome, it is likely that p105 processing is catalyzed by the 26S proteasome. In fact, Sears and Maniatis recently have identified two yeast mutants that fail to generate p50. These mutations occur in an ATPase subunit and an isopeptidase subunit that are present in the PA700 subcomplex (Sears and Maniatis, personal communication), thus providing additional support for a role of the 26S form of the proteasome in generation of p50. Appreciable evidence now indicates a close functional link between protease activity and chaperone activity in several systems, including the *Escherichia coli* ClpAP and XP proteases (Gottesman et al., 1997; Suzuki et al., 1997) and the yeast PIM1 protease (Wagner et al., 1994). Like the 26S proteasome, each of these enzymes is a large ATP-dependent protease complex and may couple ATPase activity to a process required for proteolysis. Additional work will be required to determine whether cotranslational processing of proteins by protease-chaperones is a widespread process.

Experimental Procedures

Antibodies, Enzymes, and Proteasome Inhibitors

Antibodies specific for the nuclear localization signal of p105 and the N terminus of IκB-α (C-15) were purchased from Santa Cruz Biotechnology. Antibodies specific for the influenza hemagglutinin epitope were obtained from the Berkeley Antibody Company. Antibodies reactive with the T7 gp*10* epitope tag were purchased from Novagen. Antibodies specific for Hsc70 were a gift from Dr. William Welch (University of California, San Francisco). Antibodies (E446-1) specifically recognizing the 20S proteasome were generated by the DeMartino laboratory. The proteasome inhibitor *clasto*-lactacystin β-lactone was purchased from CalBiochem, and the MG115 proteasome inhibitor was obtained from Peninsular Laboratories.

Pulse-Chase Studies

CHO-CD14 cells (Gegner et al., 1995) were seeded at 3–4 × 10^5 cells per 60 × 15 mm tissue culture dish 24 hr prior to transfection. These cells were then transfected with various expression plasmids using the LipofectAMINE reagent (GIBCO BRL). After overnight incubation, the cells were washed in phosphate-buffered saline and incubated for 1 hr at 37°C in RPMI 1640 lacking methionine and cysteine (Mediatech). Subsequently, the cells were pulse-radiolabeled by the addition of 200 μCi/ml of [^{35}S]methionine/cysteine (Du-Pont NEN) for various periods of time and chased by removal of the radiolabeled amino acids and addition of RPMI 1640 medium containing cycloheximide (12.5 μg/ml, Sigma). After defined periods of pulse or chase, the cells were lysed on ice in ELB buffer (300 mM NaCl, 0.1% Nonidet P-40, 50 mM Tris-HCl [pH 7.5], 5 mM EDTA, 1 mM phenylmethylsulfonyl fluoride, and 1 mM dithiothreitol). The lysates were centrifuged at 14,000 × g for 20 min in a refrigerated microcentrifuge to remove insoluble debris. The resulting supernatants were precleared twice with preimmune serum and protein A-Sepharose CL-4B beads (Sigma) and then immunoprecipitated with the desired antibodies and protein A-Sepharose beads. Immunoprecipitates were analyzed by 10% SDS-PAGE and fluorography. For the in vitro pulse-chase studies, cycloheximide and RNase were added to terminate the translation, and lysates were removed at various time points and immunoprecipitated in ELB buffer as described above.

In Vitro Translation

In vitro transcription and translation were performed using reagents from Promega Biotech. The desired cDNA fragments were cloned into the pET vector (Studier et al., 1990). Plasmids were linearized and transcribed using T7 RNA polymerase. Translation of the mRNAs was performed in rabbit reticulocyte lysates in the presence of 0.4 μCi/μl [^{35}S]methionine (Du Pont NEN) for varying periods of times. In experiments requiring synchronization of translation, aurintricarboxylic acid (Sigma) was added to a final concentration of 75 μM 3 min after the initiation of translation (Frydman et al., 1994). Stop buffer (20 mM Tris-HCl [pH 7.5], 5 mM $MgCl_2$, 1 mM ATP, and 2 mM puromycin) was added to the samples followed by incubation at 25°C for 5–10 min prior to immunoprecipitation.

Construction of p105 Deletion Mutants

A nested series of p105 C-terminal deletion mutants were prepared by PCR using murine p105 cDNA as a template. These cDNAs were inserted into the pEVRF mammalian expression vector as described (Lin and Ghosh, 1996). Cleavage at a unique XhoI restriction site in the p105 coding region generated a cDNA encoding an N-terminal fragment of 497 amino acids. To generate this same 497–amino acid fragment followed by an in-frame stop codon, the XhoI site was blunted using Klenow fragment and ligated to a blunted XbaI site present in the pEVRF expression vector. The mutant p105 cDNAs were also subcloned into a modified pEVRF vector (pLG033a), which contained an N-terminal 12-residue epitope tag from the T7 gp*10*. All mutations were confirmed by DNA sequencing or restriction mapping.

Immunoblotting Analysis

Lysates were prepared from CHO-CD14 cells 24–48 hr after transfection. Aliquots of these lysates were separated on 10% SDS-PAGE, transferred to Immobilon-P membranes (Millipore), and visualized by immunoblotting with specific primary antibodies and enhanced chemiluminescence (Amersham).

Acknowledgments

We thank Dr. William Welch, Dr. William Hansen, Dr. Lucy Ghoda, Dr. Romas Geleziunas, and members of our laboratories for discussions and materials. We also thank Dr. Christopher Sears and Dr. Tom Maniatis for sharing unpublished data; Dr. F. Ulrich Hartl for critical comments and William Elliston, Gary Howard, John Carroll, and Neile Shea for assistance with preparation of the manuscript and its figures. This work was supported in part by the J. David Gladstone Institutes and the University of California, San Francisco Center for AIDS Research (P30AI27763) and by National Institutes of Health grant RO1 DK46181 (G. N. D.).

Received December 31, 1997; revised February 9, 1998.

References

Baeuerle, P.A., and Baltimore, D. (1988). IκB: a specific inhibitor of the NF-κB transcription factor. Science *242*, 540–545.

Baeuerle, P.A., and Baltimore, D. (1996). NF-κB: ten years after. Cell *87*, 13–20.

Baeuerle, P.A., and Henkel, T. (1994). Function and activation of NF-κB in the immune system. Annu. Rev. Immunol. *12*, 141–179.

Baldwin, A.S., Jr. (1996). The NF-κB and IκB proteins: new discoveries and insights. Annu. Rev. Immunol. *14*, 649–683.

Beckmann, R.P., Mizzen, L.A., and Welch, W.J. (1990). Interaction of Hsp 70 with newly synthesized proteins: implications for protein folding and assembly. Science *248*, 850–854.

Beg, A.A., and Baltimore, D. (1996). An essential role for NF-κB in preventing TNF-α-induced cell death. Science *274*, 782–784.

Beg, A.A., Sha, W.C., Bronson, R.T., and Baltimore, D. (1995). Constitutive NF-kappa-B activation, enhanced granulopoiesis, and neonatal lethality in IκB-α-deficient mice. Genes Dev. *9*, 2736–2746.

Betts, J.C., and Nabel, G.J. (1996). Differential regulation of NF-κB2 (p100) processing and control by amino-terminal sequences. Mol. Cell. Biol. *16*, 6363–6371.

Blobel, G., and Sabatini, D.D. (1971). Dissociation of mammalian polyribosomes into subunits by puromycin. Proc. Natl. Acad. Sci. USA *68*, 390–394.

Chen, Z.J., Hagler, J., Palombella, V., Melandri, F., Scherer, D., Ballard, D., and Maniatis, T. (1995). Signal-induced site-specific phosphorylation targets IκBα to the ubiquitin-proteasome pathway. Genes Dev. *9*, 1586–1597.

Craiu, A., Gaczynska, M., Akopian, T., Gramm, C.F., Fenteany, G., Goldberg, A.L., and Rock, K.L. (1997). Lactacystin and *clasto*-lactacystin β-lactone modify multiple proteasome β-subunits and inhibit intracellular protein degradation and major histocompatibility complex class I antigen presentation. J. Biol. Chem. *272*, 13437–13445.

Dick, L.R., Cruikshank, A.A., Grenier, L., Melandri, F.D., Nunes, S.L., and Stein, R. (1996). Mechanistic studies on the inactivation of the proteasome by lactacystin. J. Biol. Chem. *271*, 7273–7276.

Dick, L.R., Cruikshank, A.A., Destree, A.T., Grenier, L., McCormack, T.A., Melandri, F.D., Nunes, S.L., Palombella, V.T., Parent, L.A., Plamondon, L., and Stein, R. (1997). Mechanistic studies on the inactivation of the proteasome by lactacystin in cultured cells. J. Biol. Chem. *272*, 182–188.

Donald, R., Ballard, D.W., and Hawiger, J. (1995). Proteolytic processing of NF-κB/IκB in human monocytes. J. Biol. Chem. *270*, 9–12.

Fan, C.-M., and Maniatis, T. (1991). Generation of p50 subunit of NF-κB by processing of p105 through an ATP-dependent pathway. Nature *354*, 395–398.

Fenteany, G., Standaert, R.F., Reichard, G.A., Corey, E.J., and Schreiber, S.L. (1994). A β-lactone related to lactacystin induces neurite outgrowth in a neuroblastoma cell line and inhibits cell cycle progression in an osteosarcoma cell line. Proc. Natl. Acad. Sci. USA *91*, 3358–3362.

Frydman, J., and Hartl, F.U. (1996). Principles of chaperone-assisted protein folding: differences between *in vitro* and *in vivo* mechanisms. Science *272*, 1497–1502.

Frydman, J., Nimmesgern, E., Ohtsuka, K., and Hartl, F.U. (1994). Folding of nascent polypeptide chains in high molecular mass assembly with molecular chaperones. Nature *370*, 111–117.

Gegner, J.A., Ulevitch, R.J., and Tobias, P.S. (1995). Lipopolysaccharide (LPS) signal transduction and clearance. J. Biol. Chem. *270*, 5320–5325.

Ghosh, S., Gilford, A.M., Riviere, L.R., Tempst, P., Nolan, G.P., and Baltimore, D. (1990). Cloning of the p50 DNA binding subunit of NF-κB: homology to *rel* and dorsal. Cell *62*, 1019–1029.

Goldberg, A.L. (1995). Functions of the proteasome: the lysis at the end of the tunnel. Science *268*, 522–523.

Gottesman, S., Wickner, S., and Maurizi, M.R. (1997). Protein quality by chaperones and proteases. Genes Dev. *11*, 815–823.

Hansen, W.J., Lingappa, V.R., and Welch, W.J. (1994). Complex environment of nascent polypeptide chains. J. Biol. Chem. *269*, 26610–26613.

Harhaj, E.W., Maggirwar, S.B., and Sun, S.-C. (1996). Inhibition of p105 processing by NF-κB proteins in transiently transfected cells. Oncogene *12*, 2385–2392.

Hatada, E.N., Nieters, A., Wulczyn, F.G., Naumann, M., Meyer, R., Nucifora, G., McKeithan, T.W., and Scheidereit, C. (1992). The ankyrin repeat domains of the NF-κB precursor p105 and the protooncogene bcl-3 act as specific inhibitors of NF-κB DNA binding. Proc. Natl. Acad. Sci. USA *89*, 2489–2493.

Henkel, T., Zabel, U., van Zee, K., Muller, J.M., Fanning, E., and Baeuerle, P.A. (1992). Intramolecular masking of the nuclear location signal and dimerization domain in the precursor for the p50 NF-κB subunit. Cell *68*, 1121–1133.

Henkel, T., Machleidt, T., Alkalay, I., Krönke, M., Ben-Neriah, Y., and Baeuerle, P.A. (1993). Rapid proteolysis of IκB-α is necessary for activation of transcription factor NF-κB. Nature *365*, 182–185.

Inoue, J.-I., Kerr, L.D., Kakizuka, A., and Verma, I.M. (1992). IκBγ, a 70 kd protein identical to the C-terminal half of p110 NF-κB: a new member of the IκB family. Cell *66*, 1109–1120.

Jensen, T.J., Loo, M.A., Pind, S., Williams, D.B., Goldberg, A.L., and Riordan, J.R. (1995). Multiple proteolytic systems, including the proteasome, contribute to CFTR processing. Cell *83*, 129–135.

Jentsch, S., and Schlenker, S. (1995). Selective protein degradation: a journey's end within the proteasome. Cell *82*, 881–884.

Kieran, M., Blank, V., Logeat, F., Vandekerckhove, J., Lottspeich, F., Le Bail, O., Urban, M.B., Kourilsky, P., Baeuerle, P.A., and Israël, A. (1990). The DNA binding subunit of NF-κB is identical to factor KBF1 and homologous to the rel oncogene product. Cell *62*, 1007–1018.

Komar, A.A., Kommer, A., Krasheninnikov, I.A., and Spirin, A.S. (1997). Cotranslational folding of globin. J. Biol. Chem. *272*, 10646–10651.

Krieg, U.C., Johnson, A.E., and Walter, P. (1989). Protein translocation across the endoplasmic reticulum membrane: identification by photocross-linking of a 39-kD integral membrane glycoprotein as part of a putative translocation tunnel. J. Cell Biol. *109*, 2033–2043.

Lin, L., and Ghosh, S. (1996). A glycine-rich region in NF-κB p105 functions as a processing signal for the generation of the p50 subunit. Mol. Cell. Biol. *16*, 2248–2254.

Lin, Y.-C., Brown, K., and Siebemlist, U. (1995). Activation of NF-κB requires proteolysis of the inhibitor IκB-α: signal-induced phosphorylation of IκB-α alone does not release active NF-κB. Proc. Natl. Acad. Sci. USA *92*, 552–556.

Liou, H.-C., Nolan, G.P., Ghosh, S., Fujita, T., and Baltimore, D. (1992). The NF-κB p50 precursor, p105, contains an internal IκB-like inhibitor that preferentially inhibits p50. EMBO J. *11*, 3003–3009.

Löwe, J., Stock, D., Jap, B., Zwickl, P., Baumeister, W., and Huber, R. (1995). Crystal structure of the 20S proteasome from the archaeon *T. acidophilum* at 3.4 Å resolution. Science *268*, 533–539.

Ma, C.-P., Vu, J.H., Proske, R.J., Slaughter, C.A., and DeMartino, G.N. (1994). Identification, purification, and characterization of a high molecular weight, ATP-dependent activator (PA700) of the 20S proteasome. J. Biol. Chem. *269*, 3539–3547.

MacKichan, M.L., Logeat, F., and Israël, A. (1996). Phosphorylation of p105 PEST sequences via a redox-insensitive pathway up-regulates processing to p50 NF-κB. J. Biol. Chem. *271*, 6084–6091.

Mercurio, F., DiDonato, J.A., Rosette, C., and Karin, M. (1993). p105 and p98 precursor proteins play an active role in NF-κB-mediated signal transduction. Genes Dev. *7*, 705–718.

Naumann, M., and Scheidereit, C. (1994). Activation of NF-κB *in vivo* is regulated by multiple phosphorylations. EMBO J. *13*, 4597–4607.

Naumann, M., Wulczyn, F.G., and Scheidereit, C. (1993). The NF-κB precursor p105 and the proto-oncogene product Bcl-3 are IκB molecules and control nuclear translocation of NF-κB. EMBO J. *12*, 213–222.

Netzer, W.J., and Hartl, F.U. (1997). Recombination of protein domains facilitated by co-translational folding in eukaryotes. Nature *388*, 343–349.

Orian, A., Whiteside, S., Israël, A., Stancovski, I., Schwartz, A.L., and Ciechanover, A. (1995). Ubiquitin-mediated processing of NF-κB transcriptional activator precursor p105. J. Biol. Chem. *270*, 21707–21714.

Palombella, V.J., Rando, O.J., Goldberg, A.L., and Maniatis, T. (1994). The ubiquitin-proteasome pathway is required for processing the NF-κB1 precursor protein and the activation of NF-κB. Cell *78*, 773–785.

Rechsteiner, M., Hoffman, L., and Dubiel, W. (1993). The multicatalytic and 26S proteases. J. Biol. Chem. *268*, 6065–6068.

Rice, N.R., MacKichan, M.L., and Israël, A. (1992). The precursor of NF-κB has IκB-like functions. Cell *71*, 243–253.

Rousset, R., Desbois, C., Bantignies, F., and Jalinot, P. (1996). Effects on NF-κB1/p105 processing of the interaction between the HTLV-1 transactivator TAX and the proteasome. Nature *329*, 328–331.

Scherer, D.C., Brockman, J.A., Chen, Z., Maniatis, T., and Ballard, D.W. (1995). Signal-induced degradation of IκB-α requires site-specific ubiquitination. Proc. Natl. Acad. Sci. USA *92*, 11259–11263.

Sha, W.C., Liou, H.-C., Tuomanen, E., and Baltimore, D. (1995). Targeted disruption of the p50 subunit of NF-κB leads to multifocal defects in immune responses. Cell *80*, 321–330.

Siebenlist, U., Franzoso, G., and Brown, K. (1994). Structure, regulation and function of NF-κB. Annu. Rev. Cell Biol. *10*, 405–455.

Stewart, M.L., Grollman, A.P., and Huang, M.-T. (1971). Aurintricarboxylic acid: inhibitor of initiation of protein synthesis. Proc. Natl. Acad. Sci. USA *68*, 97–101.

Studier, F.W., Rosenberg, A.H., Dunn, J.J., and Dubendorff, J.W. (1990). Use of T7 RNA polymerase to direct expression of cloned genes. Meth. Enzymol. *185*, 60–89.

Sun, S.-C., Ganchi, P.A., Béraud, C., Ballard, D.W., and Greene, W.C. (1994). Autoregulation of the NF-κB transactivator RelA (p65) by multiple cytoplasmic inhibitors containing ankyrin motifs. Proc. Natl. Acad. Sci. USA *91*, 1346–1350.

Suzuki, C.K., Rep, M., Van Dijl, J.M., Suda, K., Grivell, L.A., and States, G. (1997). ATP-dependent proteases that also chaperone protein biogenesis. TIBS *22*, 118–123.

Thanos, D., and Maniatis, T. (1995). NF-κB: a lesson in family values. Cell *80*, 529–532.

Traenckner, E.B.-M., Pahl, H.L., Henkel, T., Schmidt, K.N., Wilk, S., and Baeuerle, P.A. (1995). Phosphorylation of human IκB-α on serine 32 and 36 controls IκB-α proteolysis and NF-κB activation in response to diverse stimuli. EMBO J. *14*, 2876–2883.

Van Antwerp, D.J., Martin, S.J., Kafri, T., Green, D.R., and Verma, I.M. (1996). Suppression of TNF-α-induced apoptosis by NF-κB. Science *274*, 787–789.

Verma, I.M., Stevenson, K., Schwarz, E.W., Van Antwerp, D., and Miyamoto, S. (1995). Rel-NF-κB-IκB family: intimate tales of association and dissociation. Genes Dev. *9*, 2723–2735.

Wagner, I., Arlt, H., Van Dyck, L., Langer, T., and Neupert, W. (1994). Molecular chaperones cooperated with PIM1 protease in the degradation of misfolded proteins in mitochondria. EMBO J. *13*, 5135–5145.

Wang, C.-Y., Mayo, M.W., and Baldwin, A.S., Jr. (1996). TNF-α and cancer therapy-induced apoptosis: potentiation by inhibition of NF-κB. Science *274*, 784–787.

Watanabe, N., Iwamura, T., Shinoda, T., and Fujita, T. (1997). Regulation of NF-κB1 proteins by candidate oncoprotein BCL-3: generation of NF-κB homodimers from the cytoplasmic pool of p50-p105 and nuclear translocation. EMBO J. *16*, 3609–3620.

Weissman, J.S., Sigler, P.B., and Horwich, A.L. (1995). From the cradle to the grave: ring complexes in the life of a protein. Science *268*, 523–524.